DEVELOPMENT OF A MODEL FOR TRANSBOUNDARY FLOW

A Thesis

Presented to

the Faculty of the Department of Petroleum Engineering

University of Houston

In Partial Fulfillment

of the Requirements for the Degree

Master of Science

in Petroleum Engineering

By

Shail Apte

December 2015

DEVELOPMENT OF A MODEL FOR TRANSBOUNDARY FLOW

Shail Apte

Approved:

Dr. Kostarelos Konstantinos, Associate Professor, Chair of the Committee, Cullen College of Engineering

Committee Members:

Dr. W. John Lee, Professor Chevron Faculty Fellow, Harold Vance Department of Petroleum Engineering, Texas A&M University

Dr. Wu-Pei Su, Professor, Department of Physics

Dr. Suresh K. Khator, Associate Dean, Cullen College of Engineering

Dr. Tom Holley, Professor and Director, Petroleum Engineering Department

Acknowledgements

Firstly, I would like to express my sincere gratitude to my advisor Dr. W. John Lee for the continuous support of my thesis study and related research, for his patience, motivation, and immense knowledge. His guidance helped me in all the time of research and writing of this thesis. I could not have imagined having a better advisor and mentor for my study.

Besides my advisor, I would like to thank the rest of my thesis committee: Dr. Wu-Pei Su, and Chair of my committee Dr. Kostarelos Konstantinos, for their insightful comments and encouragement.

My sincere thanks also goes to Patrick Storer for his inputs on behavior of fractured wells. I am grateful to Prof. Chih Chen for enlightening me with the concepts of pressure transient testing, without which this research would not be possible. I thank Chenling Liao for the great discussions on flow regimes. I would also like to extend my thanks to Dr Jim Erdle for providing me with CMG.

Last but not the least, I would like to thank my family: my parents, my grandmother and my sister for supporting me spiritually throughout writing this thesis and in my life in general.

DEVELOPMENT OF A MODEL FOR TRANSBOUNDARY FLOW

An Abstract

Of a

Thesis

Presented to

the Faculty of the Department of Petroleum Engineering

University of Houston

In Partial Fulfillment

of the Requirements for the Degree

Master of Science

in Petroleum Engineering

By

Shail Apte

December 2015

Abstract

With the boom in shale plays, rate transient analysis has become the most important tool for the analysis of shales. Due to low permeability of shales, wells remain in a transient flow regime for long times (months or years) and even after several years, boundary dominated flow (usually from complete fracture interference or actual boundary) may not be observed. This prolonging of transient flow also prolongs the transition period between the end of linear flow (primary or compound linear flow) and the onset of complete boundary dominated flow, thus becoming a flow regime in itself.

This study will develop an analytical model for the transition flow regime. We expect that it will be influenced by the spacing, length, and lack of uniformity in hydraulic fracture characteristics in horizontal wells with multiple fractures. Inflow from unstimulated matrix beyond the fractured region will also influence the characteristics of this transition flow regime. We will call this flow regime the transboundary flow regime.

Table of Contents

List of Figures

Nomenclature

A_{2r}^{2n} = Mathieu function Fourier coefficients

B= formation volume factor, bbl/stb

Ce_{2n}= Radial Mathieu function

ce_{2n} = π-periodic Mathieu function

C_r= Dimensionless fracture conductivity

C_t= total compressibility, psi^{-1}

ε = Radial elliptical co-ordinate

ε_0 = Elliptical co-ordinate for boundary

Fek_{2n}= Radial Mathieu function

h= thickness of the reservoir, ft

k= permeability, md

k_f = fracture permeability, md

m(p)= Pseudo Pressure, psi2/cp

η= angular elliptical co-ordinate

p= pressure, psi

p_D = dimensionless pressure

p_D^- = dimensionless pressure in laplace space

pi= initial reservoir pressure, psi

p_{wD} = dimensionless wellbore pressure

p_{wD}^- = dimensionless wellbore pressure in laplace space

Q,q= flow rate, bbl/D, Mscf/D

q_D = Dimensionless flowrate

q_D^- = Dimensionless flowrate in laplace space

s = laplace paramtere

t= time, hrs

t_{Dxf} = dimensionless time

μ= viscosity, cp

w_f = fracture width, ft

x= Cartesian co-ordinate, ft

x_f = length of fracture, ft

x_e = distance between two fractures, ft

y = Cartesian co-ordinate, ft

y_D = dimensionless Cartesian co-ordinate

y_{eD}= dimensionless Cartesian co-ordinate for reservoir boundary

ϕ= porosity

Chapter 1 : Introduction

The recent downturn in the petroleum industry which is the result of increased supply of oil and gas, has been attributed to the boom in shale exploitation. This started due to increased energy demand worldwide which also led to continuous advances in drilling and completion techniques for the exploitation of unconventional reservoirs. Unconventional reservoirs are those that cannot be produced at economic rates without massive stimulation jobs or other recovery processes like steam injection for heavy oil reservoirs or actual mining for tar sands. SEC's (Securities and Exchange Commission) defines unconventional sources as "sources that involve extraction by means other than "traditional" oil and gas wells. These other sources include bitumen extracted from oil sands, as well as oil and gas extracted from coal and shales, even though some of these resources are sometimes extracted through wells, as opposed to mining and surface processing" (SEC,2008).

This study focuses on analyzing rate and pressure data from shale reservoirs. Shales are sedimentary rocks composed of fine grained sediments. Typically shales are source rocks which act like primary kitchens of oil and gas supplying it to a reservoir rock (e.g., sandstone or limestone), but due to the advances mentioned above it is possible to produce from them and thus act as self-sourcing reservoir rocks. Due to the ultra-low permeability of these reservoirs, it is difficult to produce economically from it using conventional methods. Recent advances in drilling and completion technology have allowed commercial exploitation of shales. Horizontal wells completed with multiple-fracturing stages

are the most widely used method for exploiting shale reservoirs. Multiple fractures help to compensate for the ultra-low permeability of these reservoirs. Therefore, development of analysis methods for analyzing production data from these wells has gained tremendous attention in the last decade.

1.1 Motivation

The most important thing for an oil company is to determine how much they can produce and how fast they can produce. To know that, it is critical to predict what the production rate is going to be in the future, how and how much is the reservoir pressure going to decline and what are the properties of a reservoir. All the above things could be predicted if we could identify and predict the flow regimes. The other challenge is to find a reasonable completion and drilling scheme in these reservoirs in order to achieve best economic result. Therefore, there is a need to develop methods which help us to identify, interpret and predict flow regimes for multiple-fractured horizontal wells. In the last decade, there has been a lot of research to develop methods for analyzing the performance of these wells and quantifying reservoir and hydraulic fracture properties. As a result, significant advances have been made in the development of different methods for rate transient analysis. As discussed by Clarkson (2013), the analysis methods that have been commonly used for shale reservoirs can be categorized as follows: 1. Straight Line Methods 2. Type Curve Methods 3. Analytical and Numerical Simulation 4. Empirical Methods 5. Hybrid Methods

The use of multiply-fractured horizontal wells is expected to create a complex sequence of flow regimes (Chen and Raghavan, 1997; Clarkson and

Pederson, 2010). The proper identification and interpretation of these flow regimes is necessary for obtaining information about the hydraulic fracture stimulation and the reservoir. Thus it is of paramount importance to construct a model for transition between different regimes for which no analytical solution exists till now.

1.2 Problem Description

In conventional reservoirs wherein pressure transient testing is performed the transition regimes last for a short duration (minutes or hours) making their analysis difficult and futile. While in unconventional reservoirs the transitions could last for days to years, which means without any model for them one would have no understanding of what is going on during such long periods of time. It also restricts one's ability to predict what would happen in future. In some of the older shale plays (e.g., Barnett) one can observe wells being in transition flow regime and with lack of an appropriate model the only thing that could be done is to fit empirical models.

In this thesis an attempt has been made to solve this problem and solutions have been provided in forms of analytical models.

1.3 Objectives

Below listed are the objectives of the present thesis:

a. To identify the flow regime between the end of primary flow and the onset of boundary dominated flow
b. To develop an analytical model for this transition flow regime
c. To develop a better way to determine flow regimes with new type curves

1.4 Organization of Thesis

The thesis is divided into 6 chapters. This chapter, Chapter 1, is the introduction and contains the motivation behind the study as well as the background to the study.

Chapter 2 presents the literature review related to the present thesis

Chapter 3 and 4 are the most important chapters in the thesis. Chapter 3 discusses different types on transitions and elaborate the combination of regimes that give rise to that transition. Chapter 4 presents the analytical solution for the transitions.

Chapter 5 deals with analysis of the presented analytical equation on simulated data

Chapter 6 discuss the application of the analytical equation on field data

Chapter 2 : Literature Review

2.1 Well Testing in Hydraulically Fracture Wells

Well testing is conducted to determine properties of the reservoir like reservoir permeability, skin, reservoir volume, reservoir pressure, determine boundaries and faults etc. It is primarily conducted by changing the flow rate of the well by closing a flowing well or an injection well respectively for buildup or falloff test or by producing well at a constant rate for a drawdown test. This change of rate creates a pressure disturbance in the reservoir which can be measured from the same well or an adjacent well in form of interference testing. Below is list of some of the well tests that exist:

• **Drawdown test**: In this test we aim to produce at constant rate while measuring the bottomhole pressure versus time. Most of the time it's unsuitable to use drawdown test data.

• **Build-up test**: In this test we are shut-in the well, thus flowing at "zero-rate" while measuring the bottomhole shut-in pressure. The well needs to be flowing for a sufficient time before it could be shut in.

• **Injection test / fall-off test**: In this process fluid is injected which lead to increase in bottomhole pressure till the fall-off period and shut-in operation is performed.

• **Interference test and pulse test**: The pressure is measured in a shut-in well which is adjacent to a producing well. This test is conducted to determine if

the two wells are connected in the reservoir or if there is a barrier between them. For pulse testing, the active well is opened for production with a number of short flow and shut-in periods, the recorded pressure vibrations are analyzed in an observation well.

In shale wells conducting a pressure transient test is unfeasible as the wells stay in transient for years so rate transient analysis is conducted instead.

Based on the test data, flow regimes could be identified. Below is the list of flow regimes typically seen in hydraulically fracture wells.

Bi-linear flow: A bi-linear flow is observed when fracture linear flow and formation linear flow exist together i.e the influence of formation linear flow could be seen on fracture linear flow. This is possible only if we have finite fracture conductivity. Bilinear flow was identified by Cinco-Ley and Sameniego (1981) by using the solution given by Cinco-Ley et al(1978). Cinco-Ley et al. (1978) in turn extended the solution presented by Gringarten et al. (1974) to investigate hydraulically fractured vertical wells with a finite conductivity vertical fracture. The equation for Bi-linear flow (Lee, 1989) is

$$p_D = \frac{1.38}{\sqrt{C_r}} t_{x_{fD}}^{\frac{1}{4}} \qquad 2.1$$

and

$$t_{x_{fD}} \frac{dp_D}{dt_{x_{fD}}} = \frac{0.345}{\sqrt{C_r}} t_{x_{fD}}^{\frac{1}{4}} \quad , \qquad 2.2$$

here

$$t_{x_{fD}} = \frac{0.0002637kt}{\phi\mu c_t x_f^2}\ , \qquad 2.3$$

$$C_r = \frac{w_f k_f}{\pi k x_f}, \qquad 2.4$$

and

$$p_D = \frac{kh\ (p_i - p)}{141.2qB\mu} \quad . \qquad 2.5$$

It can be seen from equation 2.2 that a log-log plot of pressure derivative vs time should exhibit a quarter slope when bi-linear flow exists. Generally bi-linear flow occurs during very early times and in most cases may not be seen at all, as it could get masked by wellbore storage and skin effects.

Linear flow: Linear flow exists when flow from the reservoir goes into the fracture when fracture has infinite conductivity. The equation that would represent linear flow (Lee, 1989) is given by

$$p_D = \left(\pi t_{x_{fD}}\right)^{\frac{1}{2}} \qquad 2.6$$

and

$$t_{x_{f_D}} \frac{dp_D}{dt_{x_{f_D}}} = \frac{1}{2}\left(\pi t_{x_{fD}}\right)^{\frac{1}{2}} \quad . \qquad 2.7$$

It can be seen from the equation 2.7 that a log log plot of pressure derivative vs time should give a half slope. Gringarten et al. (1975) presented type curves to analyze transient pressure behavior of infinite conductivity hydraulic fractures.

Elliptical Flow: Elliptical flow exists between linear flow and pseudo radial flow. Amini et al., 2007 gave analytical solution in laplace space for hydraulically fractured wells. But no solution in real space exists. This thesis has derived an equation for elliptical flow in real space.

In all the above cases the fluid and rock properties are assumed to be constant. This assumption does not work in cases of gases thus diffusivity equation for gases is non-linear and needs to be linearized by taking pseudo pressures. To extend the analytical solutions derived for oil to gas, Al-Hussainy and Ramey (1966) and Al-Hussainy et al. (1966) introduced the idea of real gas pseudopressure. Real gas pseudopressure is a process by which the diffusivity equation for gas is linearized using a variable transformation.

Raghavan et al. (1997) and Chen and Raghavan (1997) developed analytical pressure transient solutions for multiply fractured horizontal wells in homogeneous reservoirs. Also proposed the possibility of compound linear flow, where in a linear flow is established in the region beyond the fracture tips.

Transitions: Transitions are not well studied as they are not considered to be flow regimes. Most of them are shorter than one log cycle. Generally type curves include the transitions. The type curves for transition from primary linear flow to compound linear flow are created by Nobakht et al., 2011 and Liang et al., 2012.

Chapter 3 : Types of Transition

Transitions occur when there is a change in flow regime and thus their behavior is dictated by both the flow regimes. This implies a single model won't work in defining all kinds of transitions. But having these different models for transition regimes would help in predicting the next flow regime and could yield important properties even before the next regime starts.

3.1 Fully Penetrating fractures

A fracture penetrating the full reservoir would be here-on described as fully penetrating fracture. The flow regimes observed in such a case would be primary linear flow followed by a transition eventually leading to a boundary dominated flow(BDF). The transition in such cases can be modeled by a full solution for linear flow with a no-flow boundary condition (outer boundary condition) and with a constant pressure or constant rate at the wellbore (inner boundary condition) depending upon if rate transient analysis is being done or a pressure transient analysis. The full solution of linear flow with a rectangular boundary would exhibit no transition as shown in appendix c plot for numerical inversion of linear flow solution but a solution with non-rectangular boundary would exhibit transition. **Figure 3.1** shows a repeating block of a multiply fracture horizontal well with fully penetrating fractures.

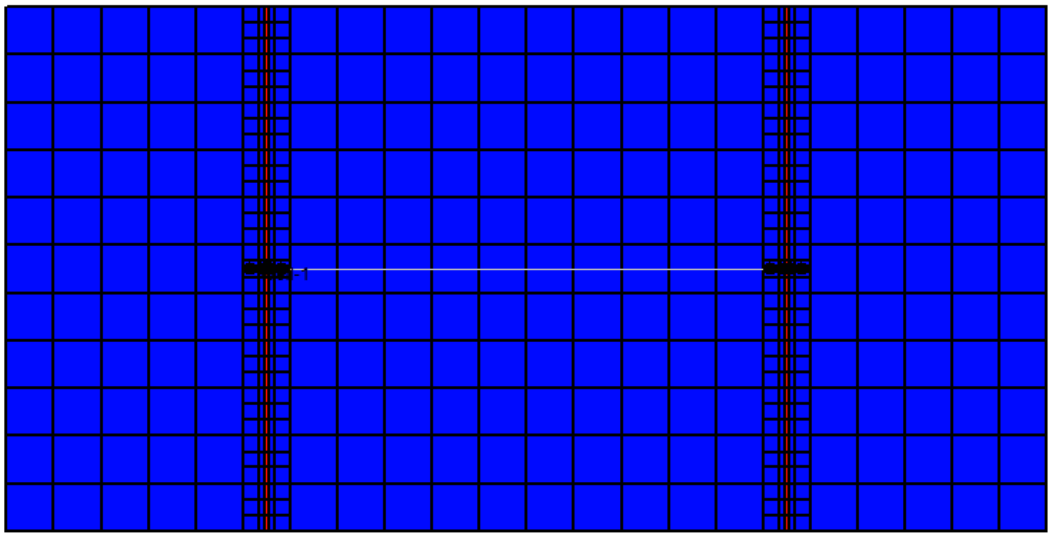

Figure 3.1: Multiply fracture horizontal well with fully penetrating fractures

Below is a representative log-log rate vs time plot for multiply fractured horizontal well with fully penetrating fractures, it can be observed that it starts with a linear flow and undergoes a short transition and ends with a boundary dominated flow. Figure 3.2 shows the dimensionless rate plot for a horizontal well with fully penetrating fractures where transition is represented by the orange section.

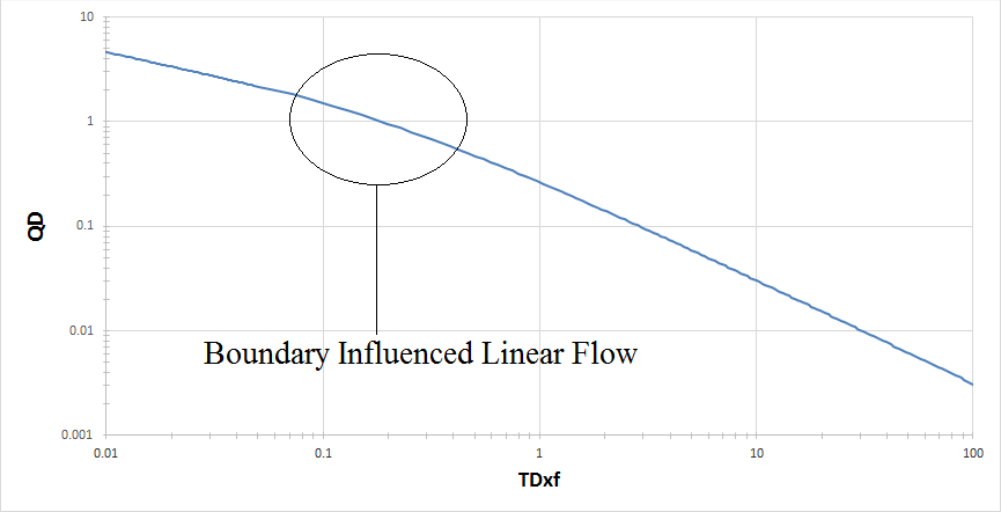

Figure 3.2: log-log dimensionless rate plot for fully penetrating fracture

Qd is dimensionless rate and T_{Dxf} is the dimensionless time

Below is the list of Regimes that would be observed in this case:

Primary flow: Linear flow

Transition 1: Boundary Influenced Linear flow

Compound flow: None

Transition 2: None

(Note: Transition 1 occurs after fracture interference and Transition 2 occurs after compound flow)

3.2 Partially Penetrating fracture

When the fractures don't completely penetrate the reservoir leaving a matrix beyond the fractures such fractures would be termed as partially penetrating fractures. Partially penetrating fractures can show multiple transitions of different types based on what the permeability difference is between the matrix and the stimulated reservoir volume(SRV) as well as how far is the boundary from the fracture tip (i.e., distance to the boundary from SRV) and if there exists space on the sides of an SRV. When we have partially penetrating fractures there is always an influence from the unstimulated matrix beyond the fracture tips. To what extent it affects would be checked in the following cases. This influence beyond from the matrix can alter the flow regime in turn altering the transition regime.

3.2.1 With SRV (Stimulated Reservoir Volume)

When the ratio of permeability of matrix to permeability of SRV is very low, the influence from beyond the fracture is minimal and could only be seen at

later times. In such cases a primary linear flow is observed which goes to transition ending up in a boundary dominated flow(due to fracture interference). Based upon the location of boundary beyond the SRV a compound flow might be observed or may not be observed. Also this compound flow can be either an elliptical flow or a linear flow based on if there exists space on the sides of SRV. This compound flow will eventually transition to a BDF (due to actual reservoir boundary) when the reservoir boundary is seen. Now the model for transition from compound flow to BDF would be influenced by the type of compound flow namely elliptical or linear.

a) When the reservoir boundary is near

When the reservoir boundary is near we would observe an elliptical flow after fracture interference. The elliptical flow will transition into BDF (due to reservoir boundary).

Figure 3.3 shows a horizontal well with partially penetrating fractures with SRV and a close reservoir boundary. The green colored region represents SRV while the blue section is unstimulated matrix.

The elliptical flow includes two specific sections which can be termed as different flow regimes which would be discussed in subsequent chapters. The boundary influenced elliptical flow which is a flow regime where in boundary has been seen would be discussed in later chapters. This particular flow regime would not be seen when we encounter a situation similar to present case with reservoir boundary being very near.

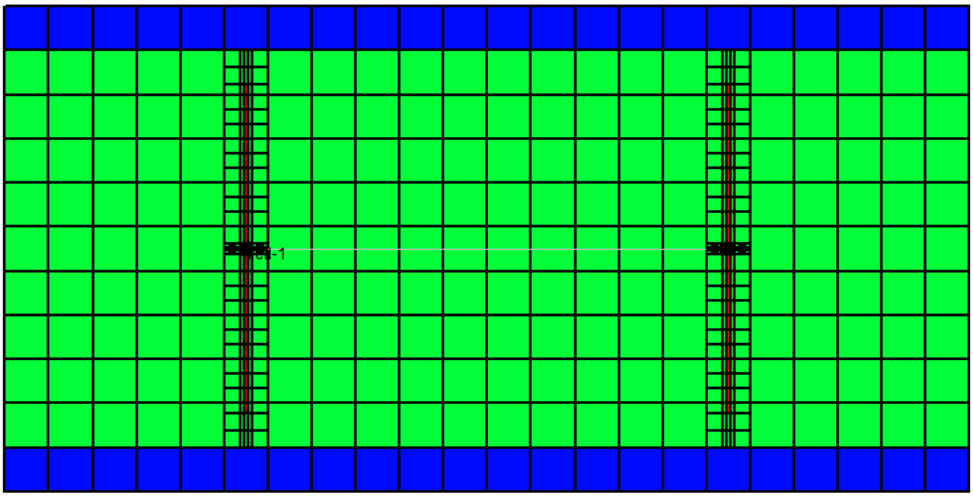

Figure 3.3: Partially penetrating fractures with SRV and a near boundary

The transition from fracture interference to BDF (reservoir boundary) can be divided in two parts first being sustained elliptical flow and second being boundary influenced elliptical flow. Both of these would be discussed in subsequent chapters.

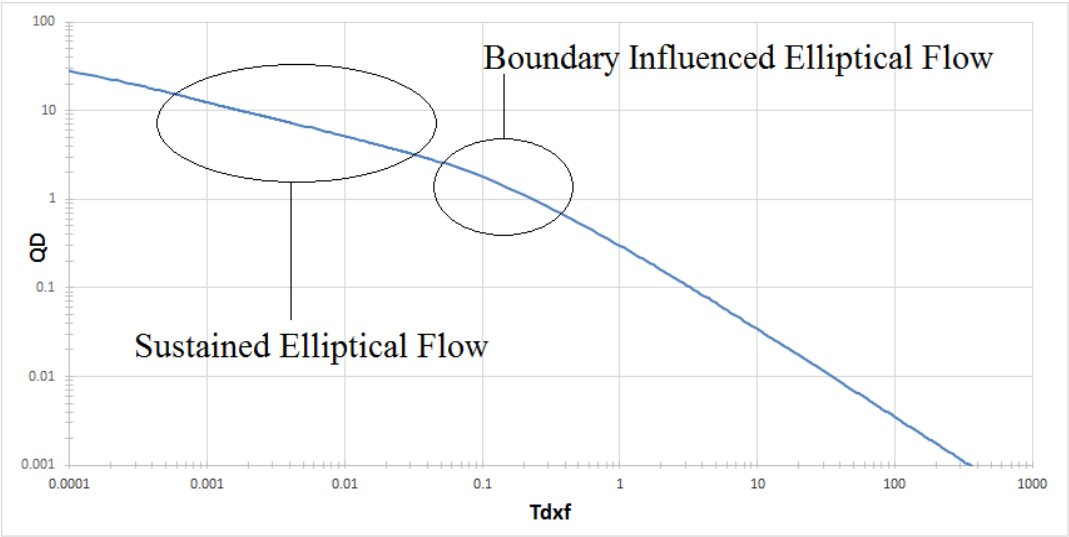

Figure 3.4 : Log log Dimensionless rate vs dimensionless time plot for partially penetrating fracture with near reservoir boundary

Below is the list of Regimes that would be observed in this case:

Primary flow: Linear flow

Transition 1: Elliptical flow followed by Boundary influenced elliptical flow

Compound flow: None

Transition 2: None

b) When the reservoir boundary is far

When the reservoir boundary is far a transition from fracture interference to compound flow can be observed. This transition is primarily sustained elliptical flow. This elliptical flow could be sustained and become compound elliptical flow if there is support from sides of SRV or would turn into compound linear flow if there is no support from sides of the SRV. This compound flow will then transition to BDF (reservoir boundary). This transition can be modeled with boundary influenced linear flow or boundary influenced elliptical flow based on the compound flow regime.

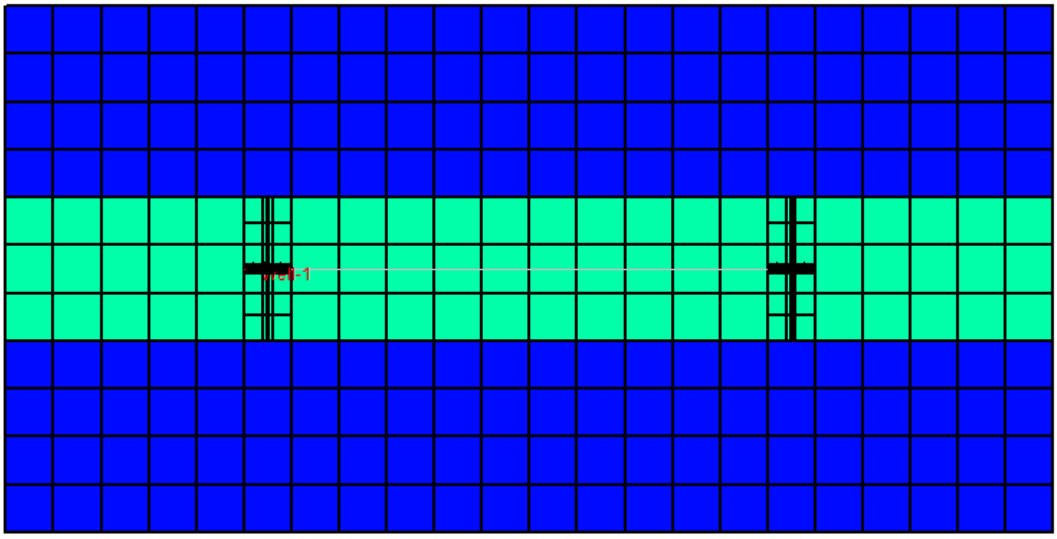

Figure 3.5: Horizontal well with partially penetrated fractures with SRV and a far boundary

Case 1: There exists no space beyond the SRV

Below is the list of Regimes that would be observed in this case:

Primary flow: Linear flow

Transition 1: Elliptical flow

Compound flow: Linear flow

Transition 2: Boundary Influenced linear flow

Case 2: There exists space beyond the SRV

Below is the list of Regimes that would be observed in this case:

Primary flow: Linear flow

Transition 1: Elliptical flow

Compound flow: Sustained Elliptical flow

Transition 2: Boundary Influenced Elliptical flow

3.2.2 Without SRV

When the permeability of SRV and the unstimulated matrix is very similar it can treated as if there is no SRV and with a partially penetrated fracture, the flow regime is primarily elliptical. The transition to BDF (fracture interference) would thus be boundary influenced elliptical flow. After fracture interference either a compound elliptical or compound linear flow would be observed depending upon if there exists space on the side of the horizontal well in the direction of the horizontal well.

a) If there exists space on the side of the horizontal well

If there exists space on the side of the horizontal well the compound flow would most likely be elliptical in nature. And the transition from compound

elliptical flow to BDF (reservoir boundary) is going to be boundary influenced elliptical flow. **Figure 3.6** shows a multiply fracture horizontal well with partially penetrating fractures and having space beyond the horizontal well.

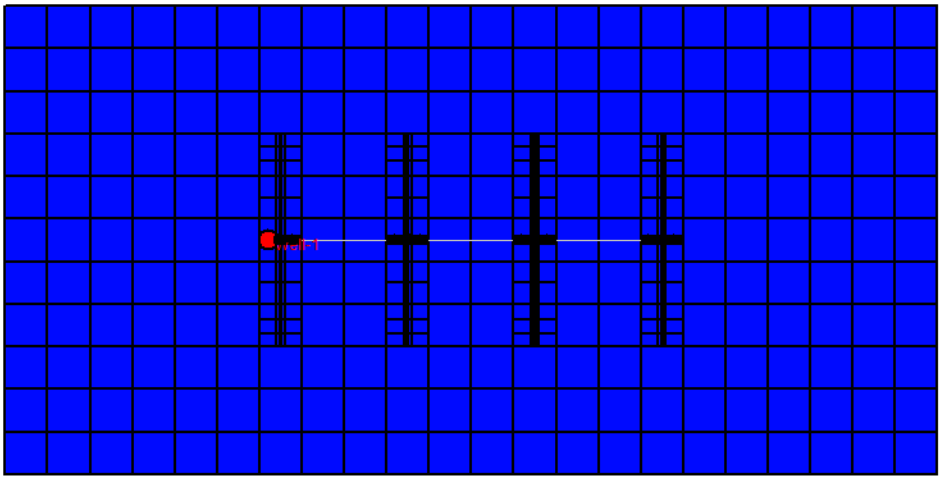

Figure 3.6: Multiply fractured horizontal well with partially penetrating fracture and space on the sides of horizontal well

Below is the list of Regimes that would be observed in this case:

Primary flow: Linear flow followed by Elliptical flow

Transition 1: Elliptical flow

Compound flow: Elliptical flow

Transition 2: Boundary Influenced Elliptical flow

b) If there exists no space on the side of the horizontal well

If there exists no space on the side of the horizontal well the compound flow would most likely be linear flow and the transition to BDF(reservoir boundary) can be described by boundary influenced linear flow which can be extracted empirically from full linear flow solution.

Figure 3.7 shows a multiply fractured horizontal well with partially penetrating fractures and no space on the side of the horizontal well.

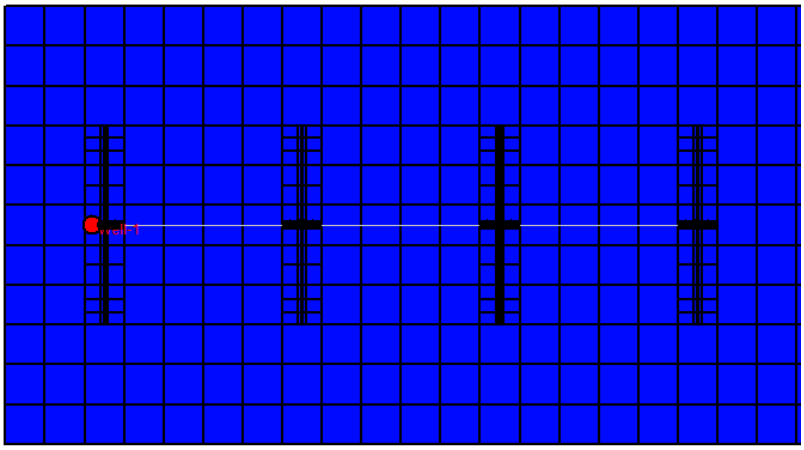

Figure 3.7 : Multiply fractured horizontal well with partially penetrating fractures and no space on the side of the horizontal well

Below is the list of Regimes that would be observed in this case:

Primary flow: Linear flow followed by Elliptical flow

Transition 1: Elliptical flow

Compound flow: Linear flow

Transition 2: Boundary Influenced Linear flow

Note: Only broad and limited cases have been discussed in this chapter, multiple more cases can be made and analyzed.

Chapter 4 : Model Development

The full solutions in Laplace space with constant pressure/constant rate inner boundary condition and no flow outer boundary condition for the cases of elliptical flow and linear flow is presented in Appendix A and Appendix B respectively. These solutions can be easily inverted using numerical methods, while analytical inversion poses difficulties. The analytical inversion of elliptical flow solution is not available and thus this chapter tries to determine the equations in real space for sustained elliptical flow and boundary influenced elliptical flow using short time and longtime approximation. A matlab code for numerical inversion is provided in Appendix-C.

4.1 Sustained Elliptical Flow

Sustained Elliptical flow is the region where elliptical flow can be clearly observed. As elliptical flow moves further away it turns into radial flow as the nature of elliptical flow cannot be observed when the flow is coming from a farther distance. In an infinite acting reservoir outer boundary condition elliptical solution the region up to which elliptical flow can be observed would be termed as Sustained Elliptical flow. Analytical inversion of the full solution of both infinite acting and no-flow boundary reservoirs is difficult and thus a semi-analytical inversion using short time approximation on a no-flow outer boundary condition reservoir and constant pressure inner boundary would be conducted and equation for sustained elliptical flow would be obtained.

The pressure solution for sustained elliptical flow for a constant rate case can be given as

$$p_{wD} = \left(\frac{\left(\frac{\pi \sinh(2\epsilon_0)}{2} \right)^{-\frac{3}{8}}}{\left(e^{-\left(\frac{3}{4}\right)\epsilon_0} \right)} \right) \sin\left(\frac{3\pi}{8}\right) t_{Dxf}^{\frac{3}{8}} \quad . \tag{4.1}$$

And a rate solution for constant bottomhole pressure can be given as

$$q_D = \left(\frac{8}{3\pi}\right)\left(e^{-\left(\frac{3}{4}\right)\epsilon_0} \right) \frac{t_{Dxf}^{-\frac{3}{8}}}{\left(\frac{\pi \sinh(2\epsilon_0)}{2} \right)^{-\frac{3}{8}}} \quad , \tag{4.2}$$

where 4.3

$$\epsilon_0 = \sinh^{-1}\left(\frac{x_e}{2x_f}\right)$$

and x_e is distance between fractures and x_f is fracture half length.

The behavior of the following term

$$FH = \frac{\left(\frac{8}{3\pi}\right)\left(e^{-\left(\frac{3}{4}\right)\epsilon_0} \right)}{\left(\frac{\pi \sinh(2\epsilon_0)}{2} \right)^{-\frac{3}{8}}} \tag{4.4}$$

is very unique and for ε_0 values greater than 2 it can assumed to be a constant of value 0.775314.

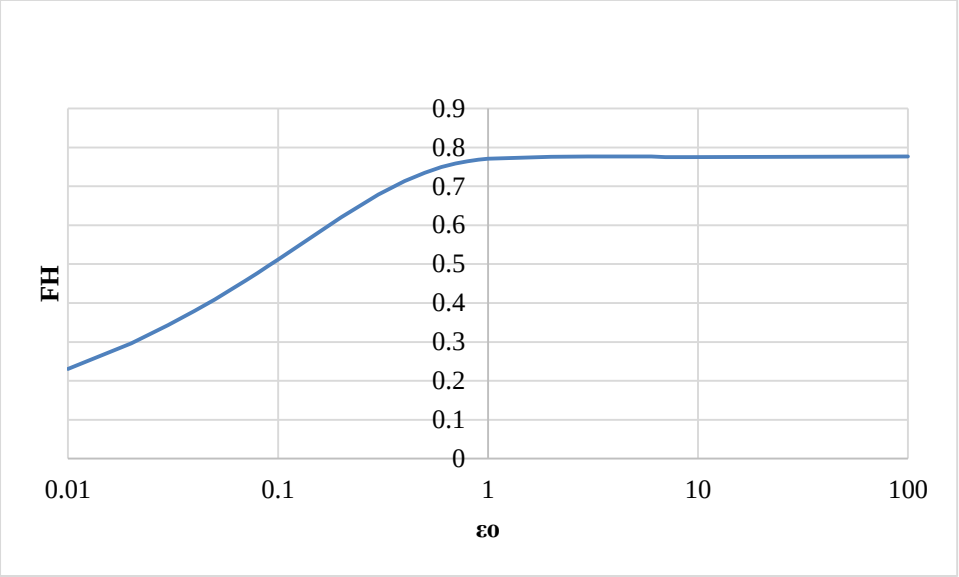

Figure 4.1: Relation between FH and ε_0

From the above plot ε_0 of 1 translates to x_e/x_f of 2.35 i.e for xe/xf>2.35 ε_0 is a constant. Based on the above the equations for Pw_D and Q_D can be written as

$$p_{wD} = 1.011478\, t_{Dxf}^{\frac{3}{8}} \qquad 4.5$$

and

$$q_D = 0.775314\, t_{Dxf}^{-\frac{3}{8}} \qquad 4.6$$

for the case of ε_0 greater than 1.

Note: The above equations are only valid for xe/xf>2.35, in case this condition is not satisfied use the full equations with ε_0 as mentioned in equation 4.1 and equation 4.2.

4.2 Boundary Influenced Elliptical Flow

The transition from elliptical flow to boundary dominated flow is termed as boundary influenced elliptical flow, the region can be identified in full solution of elliptical flow for a case of no-flow boundary. The equation for the same is

$$q_D = \left(\frac{9}{\pi^4}\right)\left(1 + \left(\frac{2\pi}{3}\right)e^{-\left(\frac{3}{4}\right)\epsilon_0}\right)\frac{t_{Dxf}^{-\frac{2}{3}}}{\left(\frac{\pi \sinh(2\epsilon_0)}{2}\right)^{-\frac{2}{3}}} \qquad 4.7$$

for a rate solution with constant bottom hole pressure and

$$p_{wD} = \left(\frac{\left(\frac{\pi \sinh(2\epsilon_0)}{2}\right)^{-\frac{2}{3}}}{\left(\frac{6}{\pi^3}\right)\left(1 + \left(\frac{2\pi}{3}\right)e^{-\left(\frac{3}{4}\right)\epsilon_0}\right)}\right)\sin\left(\frac{2\pi}{3}\right) t_{Dxf}^{\frac{2}{3}} \qquad 4.8$$

for a pressure solution with constant rate.

Equations 4.2 and 4.7 are solutions of equation A.28 for early intermediate and late intermediate times respectively.

4.3 Boundary Influenced Linear Flow

The transition from linear flow to boundary dominated flow is termed as boundary influenced linear flow, the region cannot be identified in full solution of linear flow for a case of no-flow boundary as it is too short to be observed in an analytical solution. But it can be observed in simulations where the boundary is non rectangular for a linear flow. The equation for the same has not been derived

in the present thesis and more work is needed to determine an analytical solution. But its behavior can be identified as probably exhibiting a slope of ¾ as observed from the simulation data. The full linear flow solution inversion is shown in Appendix-C in the figure C.2. It can be observed in this inversion that no transition exists even when we have higher distance to the boundary. This shows that it would be difficult to define the transition unless the coordinate system transformed to account for non-rectangular boundary.

Chapter 5 : Validation on Simulated Results

Chapter 3 deals with types of transitions and Chapter 4 gives equations for different flow regimes which combined together forms different kinds of transitions. In this chapter we would apply them on simulated data to check if it actually works.

5.1 Boundary Influenced Elliptical Flow Transition

Below are simulations which exhibit a boundary influenced elliptical flow transition. Most of the transitions don't comprise of full log cycles and won't be called a flow regime while if we look at them in terms of time for a typical shale well, they last for 3 to 10 years which is large enough in time domain though it's not a full log cycle.

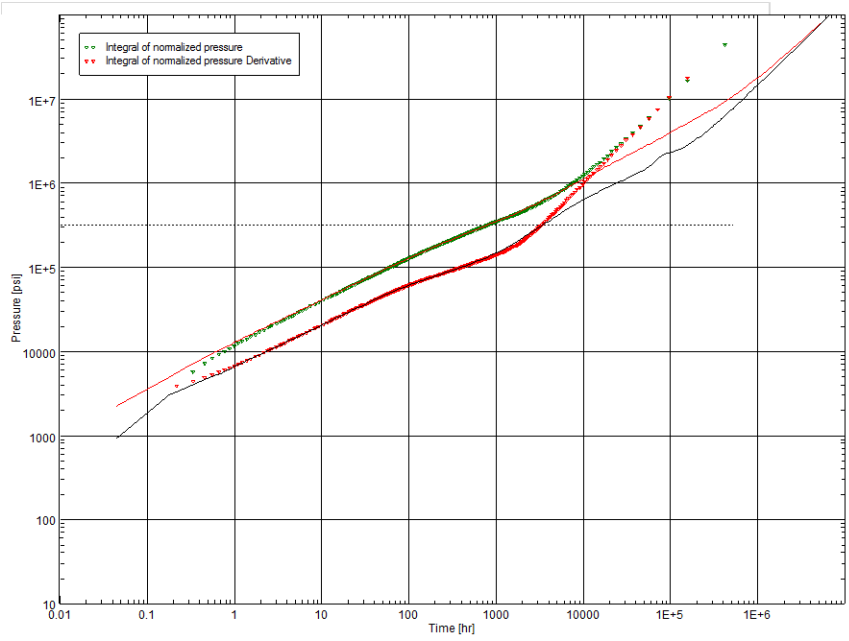

Figure 5.1: Log-log plot of pressure & derivate vs time for cases of near and far boundaries for a fractured well in a rectangular reservoir

The figure 5.1 shows two simulation cases, the dotted one signifying a near boundary case while the solid line showing the far boundary case. It can be observed from this, that a near boundary case doesn't exhibit a boundary influenced elliptical flow. This is because it is very short on a log-log plot. The far boundary case exhibits a boundary influenced elliptical flow for a very long period and can be easily identified in the log-log plot as the section exhibiting a 2/3 slope. Below figure shows the boundary influenced elliptical flow for the far boundary case using the blue line.

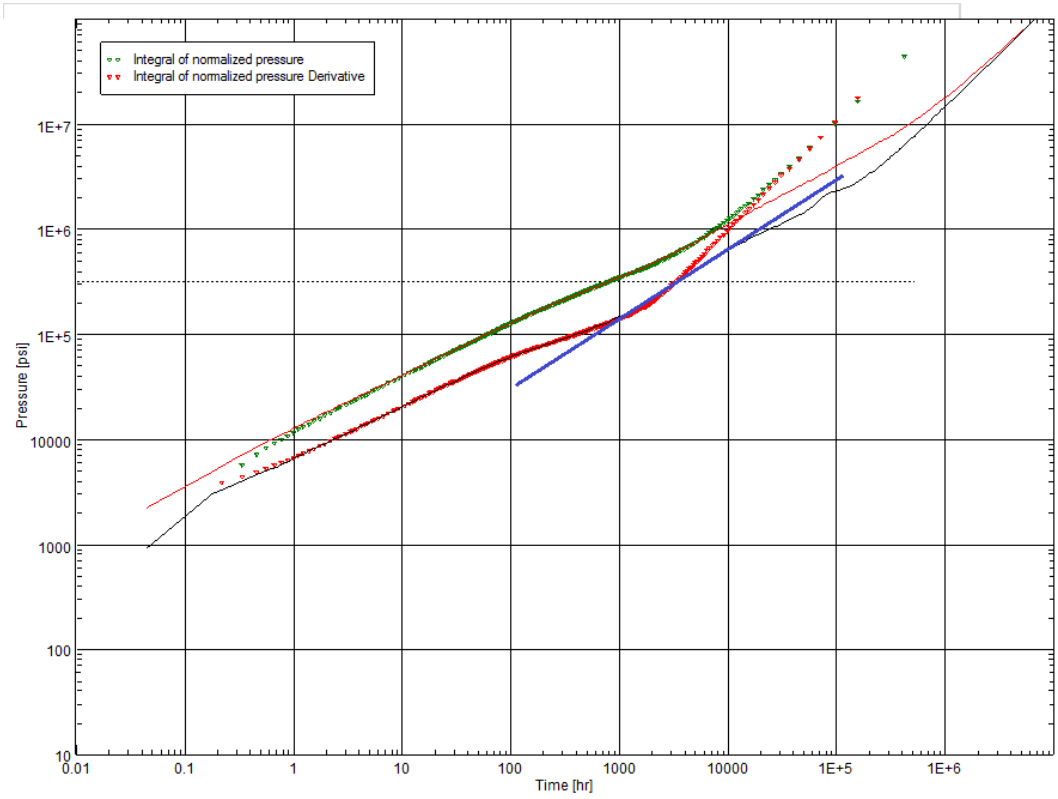

Figure 5.2: Log-log plot of pressure & derivate vs time showing boundary influenced elliptical flow (blue line-2/3 slope)

5.2 Sustained Elliptical Flow Transition

A sustained elliptical flow would be present before a boundary influenced elliptical flow. Thus the transition would be divided in 2 parts elliptical flow and boundary influenced elliptical flow. Below are the cases that exhibit a sustained elliptical flow transition. An elliptical flow would either exist in place of a linear flow or after a linear flow period.

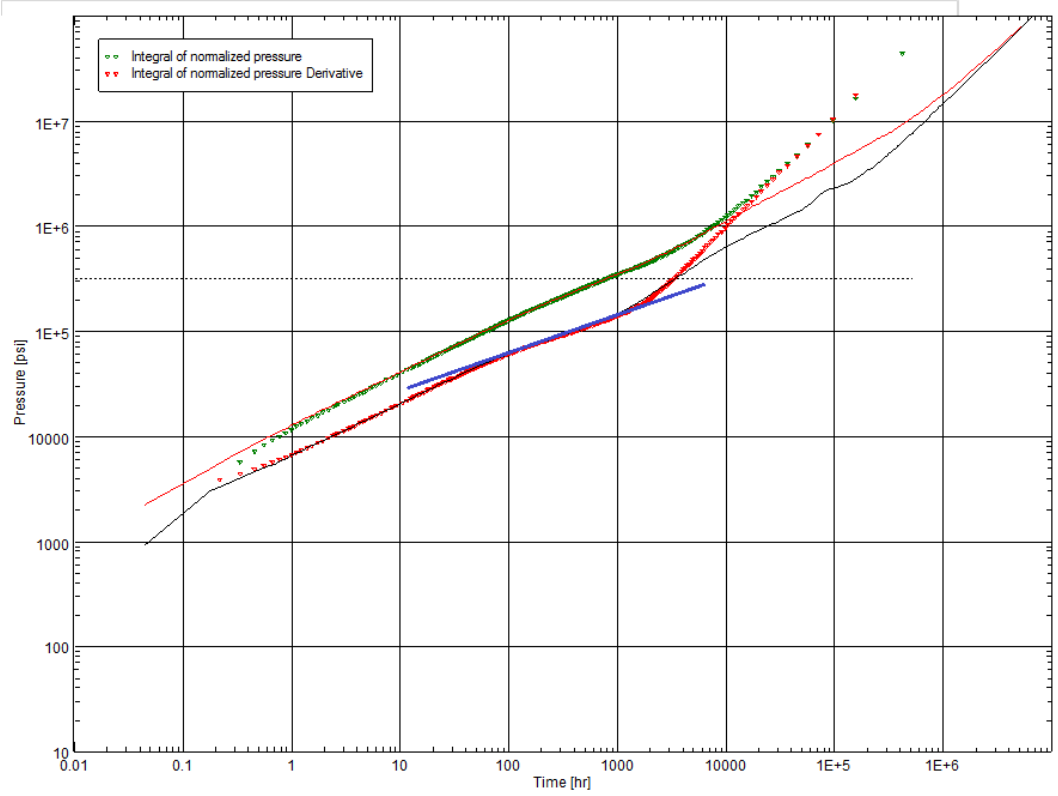

Figure 5.3: Log-log plot of pressure & derivate vs time showing sustained elliptical flow (blue line-3/8 slope)

It can be seen that in both the cases i.e, when boundary is near or far the linear flow is followed by sustained elliptical flow.

Chapter 6 : Application on Field Results

In this chapter the flow regimes described earlier would be applied on field data to yield properties such as permeability and fracture half length.

Below described is shale well with 12 fractures and lateral length of 3900 ft.

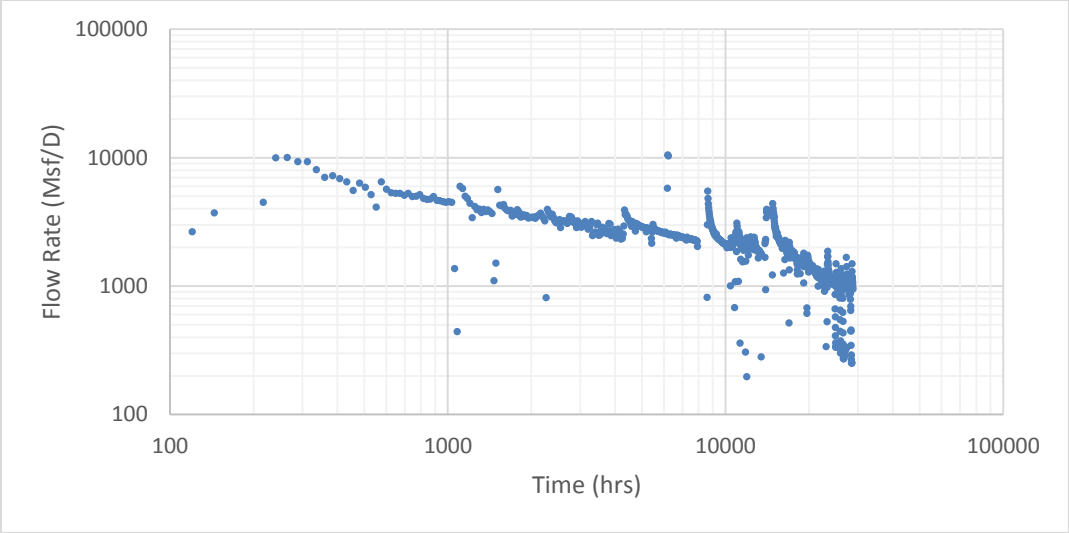

Figure 6. 1: Rate vs time plot for a shale well

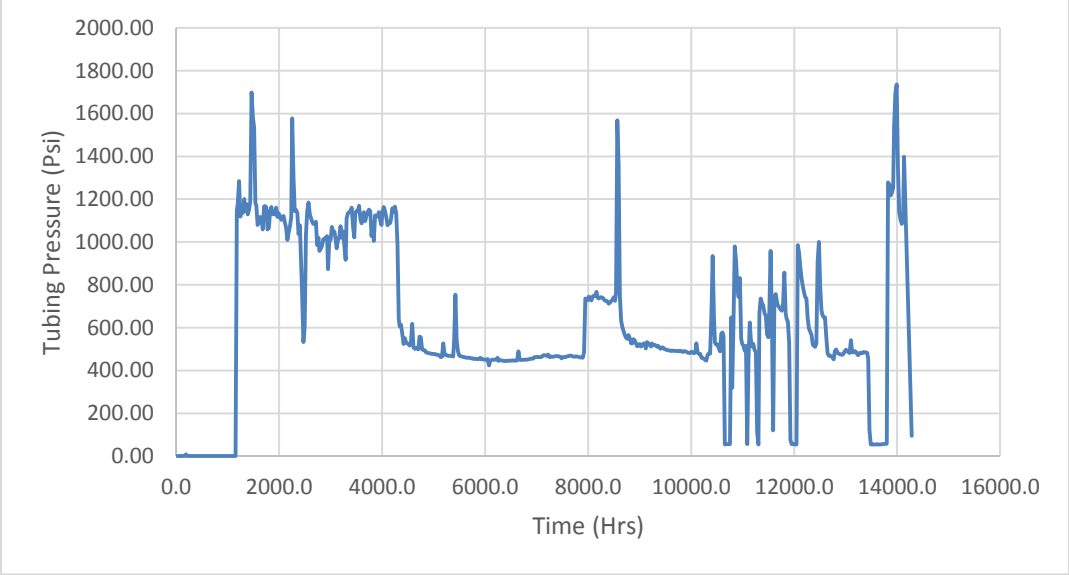

Figure 6. 2: Pressure vs time plot for a shale well

It can be observed from the rate plot above that the well exhibits a sustained elliptical flow behavior. Below is the plot showing the sustained elliptical flow behavior.

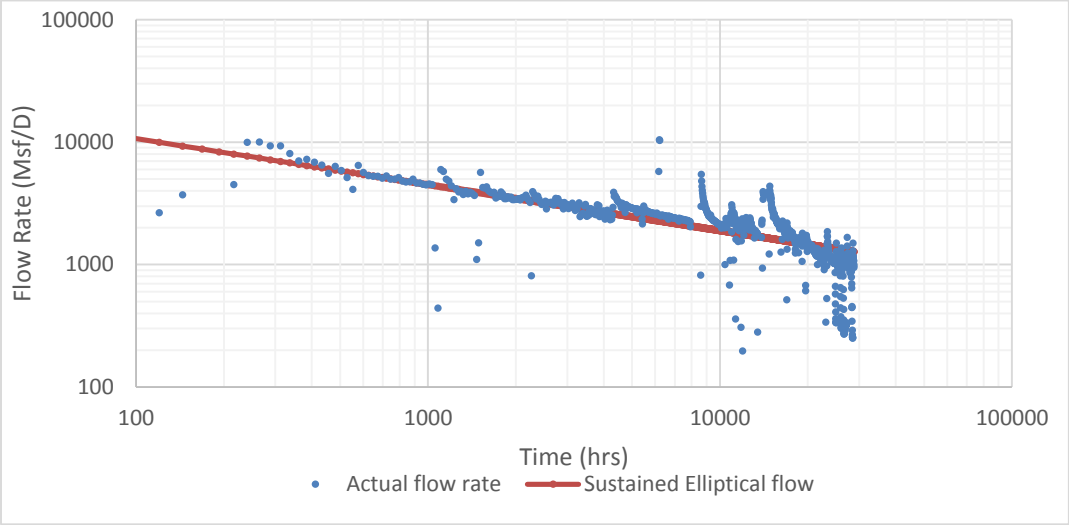

Figure 6. 3: Sustained elliptical flow on the rate plot of shale well

Applying equation 4.6 on the above plot we determine that

$$\frac{1422Tq}{kh\Delta m(p)} = 0.77534(t)^{-\frac{3}{8}}\left(\frac{0.0002637k}{\phi\mu c_g x_f^2}\right)^{-\frac{3}{8}}, \qquad 6.1$$

where

$$\frac{1422Tq}{kh\Delta m(p)} = q_D \quad . \qquad 6.2$$

Solving equation 6.1 for the present case gives the relationship

$$k^{\frac{5}{8}} x_f^{\frac{3}{4}} = 0.64 \quad . \qquad 6.3$$

This gives the following values for xf (ft) and k(md)

Xf= 100 (ft) would be k=0.00194 md

Xf=200 (ft) would be k=0.00084 md

Xf=300 (ft) would be k=0.00052 md

Thus sustained elliptical flow can be used in the same way as linear flow which yields a relationship k and xf.

Another workflow to determine k and xf relationship can also be used where in once you have identified the line with slope of 3/8 extrapolate it to time t=1 hour and use the intercept in the equation given as

$$Intercept = 0.77534\left(\frac{0.0002637k}{\phi\mu c_g x_f^2}\right)^{-\frac{3}{8}}\left(\frac{kh\Delta m(p)}{1422T}\right) \quad . \qquad 6.4$$

Below is the rate vs time log-log plot for another well.

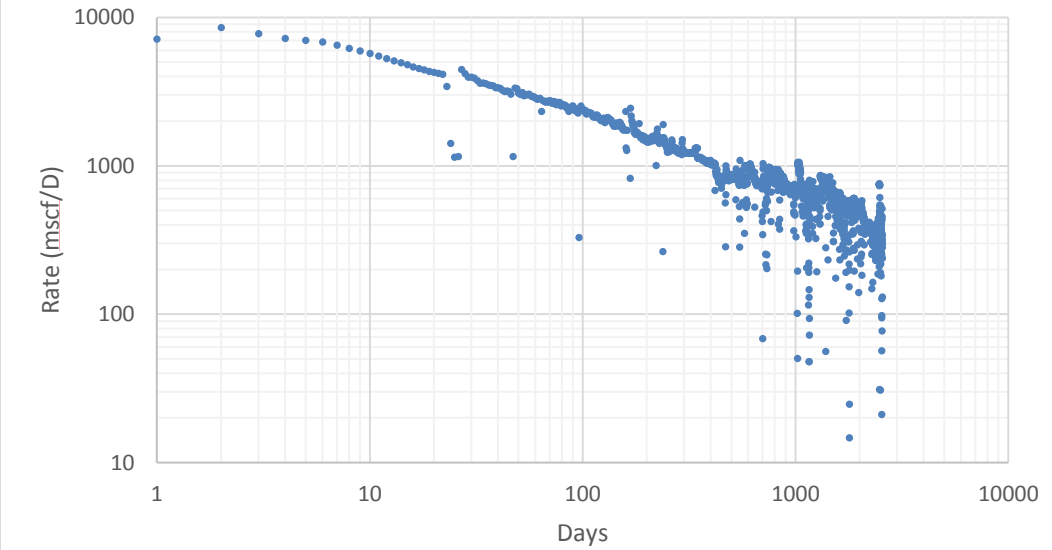

Figure 6. 4: Rate vs time plot for well2

The above plot shows both the flow regimes of sustained elliptical flow and boundary influenced elliptical flow as shown in the plot below

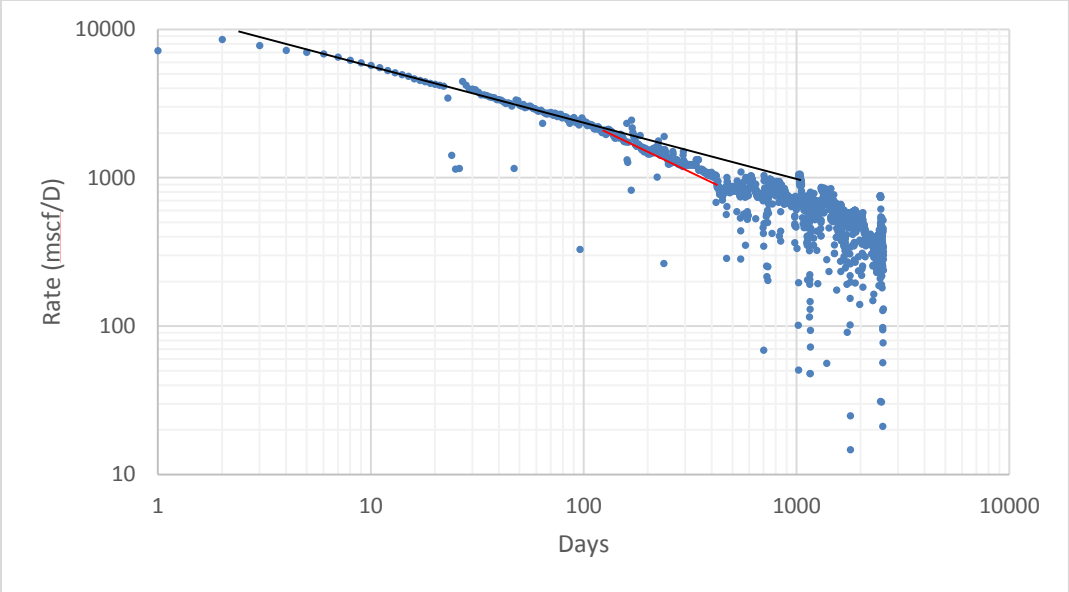

Figure 6. 5: log-log rate vs time here, black line: Sustained elliptical flow, Red line: Boundary influenced elliptical flow

If fracture spacing is known then the following procedure can be used to determine the start time of boundary influenced elliptical flow which can be given as

$$t_{Dxf}^{-\frac{7}{24}} = \frac{0.775314\left(\frac{\pi\, sinh(2\epsilon_0)}{2}\right)^{-\frac{2}{3}}}{\left(\frac{9}{\pi^4}\right)\left(1+\left(\frac{2\pi}{3}\right)e^{-\left(\frac{3}{4}\right)\epsilon_0}\right)} \quad . \qquad 6.5$$

Thus allowing us to predict when boundary influenced elliptical flow will start, this has big implication on future rate predictions. So as soon as we observe sustained elliptical flow we can calculate when boundary influenced elliptical flow will start and boundary influenced elliptical flow lasts only for 1 log cycle and thus based on distance between two parallel horizontal wells we can predict which flow regime would show up after boundary influenced elliptical flow and thus all future rates can be accurately predicted.

Chapter 7 : Results

The Results of the thesis can be broadly stated as listed below:

- Transitions for fractured wells (vertical or horizontal) are combinations of sustained elliptical flow, boundary influenced elliptical flow and boundary influenced linear flow.
- Sustained elliptical flow would exist in place of linear flow or will occur after a linear flow for the case of primary linear flow.
- Sustained elliptical flow can be identified by the slope of 3/8 on a log-log plot of rate vs time or pressure derivative vs time
- Boundary influenced elliptical flow would occur only if sustained elliptical flow exists before it.
- Boundary influenced elliptical flow can be identified by the slope of 2/3 on a log-log plot of rate vs time or pressure derivative vs time
- Information about extent of the reservoir can be determined from boundary influenced elliptical flow
- Boundary influenced linear flow would occur only if linear flow exists before it. And it can probably be identified by 3/4 slope on a log-log plot of rate vs time or pressure derivative vs time.

References

Al-Hussainy, R., and Ramey, H. J. 1966. "Application of Real Gas Theory to Well Testing and Deliverability Forecasting." *JPT* **18** (5): 637-642. SPE 1243-PA.

Al-Hussainy, R., Ramey, H. J., and Crawford, P. B. 1966. "The Flow of Real Gases through Porous Media." *JPT* **18** (5): 624-636. SPE 1243-A.

Amini, S., Ilk, D., and Blasingame, T.A. 2007. "Evaluation of the Elliptical Flow Period for Hydraulically-Fractured Wells in Tight Gas Sands-Theoretical Aspects and practical Considerations." Paper SPE 106308 presented at the SPE Hydraulic Fracturing Technology Conference, College Station, Texas, USA,29-31 January. http://dx.doi.org/10.2118/106308-MS

Chen, C.C. and Raghavan, R. 1997. "A Multiply-Fractured Horizontal Well in a Rectangular Drainage Region." *SPE J.* **2** (4): 455–465. SPE-37072-PA. DOI: 10.2118/37072-PA.

Cinco, L. H., and Sameniego, V. F. 1981. "Transient Pressure Analysis for Fractured Wells." *JPT* **33** (9): 1749-1766. SPE 7490-PA.

Cinco, L. H., Sameniego, V. F., and Dominguez, A. N. 1978. "Transient Pressure Behavior for a Well with a Finite-Conductivity Vertical Fracture." *SPEJ* 18 (4): 253-264. SPE 6014-PA.

Clarkson, C.R. and Pedersen, P.K. 2010. "Tight Oil Production Analysis: Adaptation of Existing Rate-Transient Analysis Techniques." Paper SPE 137352

presented at the Canadian Unconventional Resources and International Petroleum Conference, Calgary, Alberta, 19–21 October. DOI: 10.2118/137352-MS.

Clarkson, C.R. 2013. "Production data analysis of unconventional gas: Review of theory and best practices." *International Journal of Coal Geology* **109–110**:101–146. DOI:10.1016/j.coal.2013.01.002.

Gringarten, A. C. and Ramey, H. J., and Raghavan, R. 1974. "Unsteady-State Pressure Distributions Created by a Well with a Single Infinite-Conductivity Vertical Fracture." *SPEJ* 14 (4): 347-360. SPE 4051-PA.

Gringarten, A. C. and Ramey, H. J., and Raghavan, R. 1975. "Applied Pressure Analysis for Fractured Wells." *JPT* **27** (7): 887-892. SPE 5496-PA.

Kucuk, F and Brigham, William E. 1979. "Transient flow in elliptical systems." *SPEJ*, SPE7488

Lee, W.J. 1989. "Postfracture Formation Evaluation." In Recent Advances in Hydraulic Fracturing, J.L. Gidley, S.A. Holditch, D.E. Nierode, and R.W. Veatch Jr. eds., Vol. 12. Richardson, Texas: Monograph Series, SPE.

Liang, P., Thompson, J. M. and Mattar, L. 2012. "Importance of the Transition Period to Compound Linear Flow in Unconventional Reservoirs." SPE 162646-MS MS presented at the Canadian Unconventional Resources Conference, Calgary, Alberta, 30 Oct-1 November

Nobakht, M. ,Clarkson, C. R. and Kaviani, D. 2011. "New Type Curves for Analyzing Horizontal Well With Multiple Fractures in Shale Gas Reservoirs." SPE

149397-MS presented at the Canadian Unconventional Resources Conference, Calgary, Alberta, 15-17 November

Raghavan, R. S., Chen, C. and Agarwal, B. 1997. "An Analysis of Horizontal Wells Intercepted by Multiple Fractures." *SPEJ* **2** (3): 235-245. SPE 27652-PA.

SEC, 2008. "Modernization of Oil and Gas Reporting," http://www.sec.gov/rules/final/2008/33-8995.pdf

Stehfest, H., 1970, Algorithm 368: "Numerical inversion of Laplace transform," *Communication of the ACM*, vol. 13 no. 1 p. 47-49

Villinger, H., 1985, "Solving cylindrical geothermal problems using Gaver-Stehfest inverse Laplace transform," *Geophysics*, vol. 50 no. 10 p. 1581-1587

Appendix-A

Derivation of elliptical flow model:

Elliptical flow solutions can be derived by converting the diffusivity equation into elliptical co-ordinate system.

Following is the diffusivity equation in Cartesian co-ordinates

$$\frac{\partial^2 p}{\partial x^2} + \frac{\partial^2 p}{\partial y^2} = \frac{\phi \mu c_t}{k}\left(\frac{\partial p}{\partial t}\right) . \qquad \text{A.1}$$

The assumptions for this equation are:

1) Isotropic, homogenous, horizontal reservoir with uniform thickness of h, porosity of ϕ, permeability of k.
2) The total compressibility of the system is c_t and the reservoir fluid is slightly compressible and the viscosity of the fluid is μ.
3) There is no gravity effect and the flow inside the reservoir is laminar

Now to transform the above Cartesian diffusivity equation into elliptical co-ordinates we use the following transformation:

$$x = x_f \sinh(\epsilon) \sin(\eta) \qquad \text{A.2}$$

and

$$y = x_f \cosh(\epsilon) \cos(\eta) . \qquad \text{A.3}$$

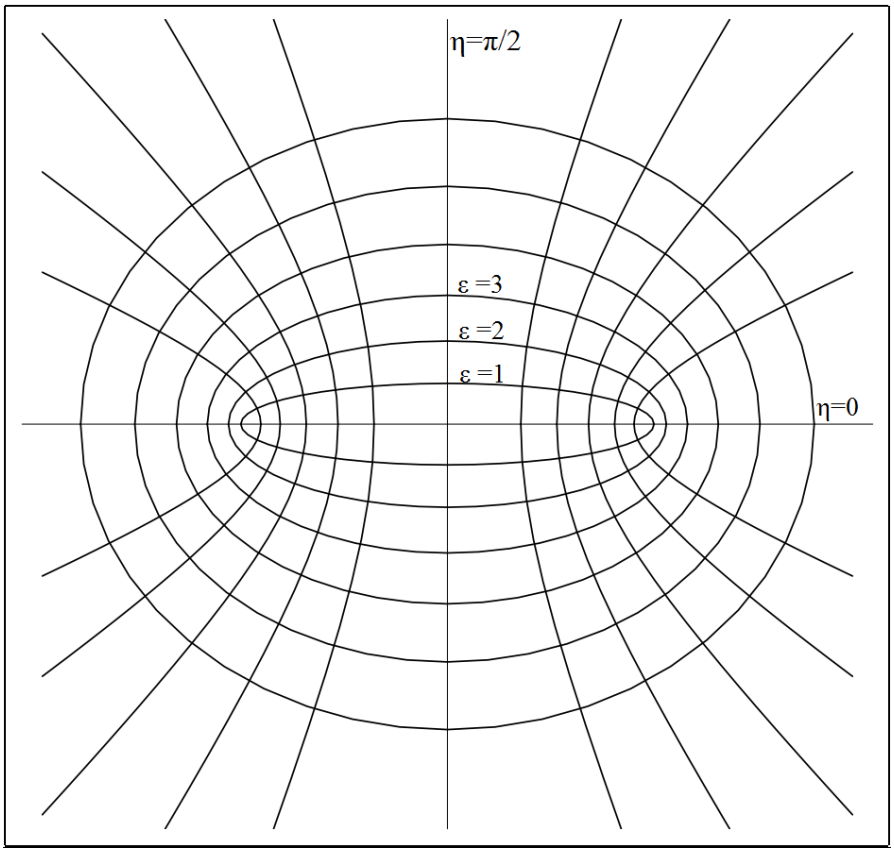

Figure A. 1: Elliptical co-ordinates

As shown above here ε represents a family of confocal ellipses. The focal length of these ellipses is $2x_f$. The η represents a family of confocal hyperbolas. The co-ordinates ε and η are orthogonal to each other. The transformed diffusivity equation is

$$\frac{\partial^2 P}{\partial \epsilon^2} + \frac{\partial^2 P}{\partial \eta^2} = \frac{\phi \mu c_t x_f^2}{2k} (\cosh(2\epsilon) - \cos(2\eta)) \frac{\partial p}{\partial t} \quad . \qquad \text{A.4}$$

Now converting the above equation in dimensionless form using the following:

$$p_D = \frac{p_i - p}{p_i - p_{wf}} \qquad \text{A.5}$$

and

$$t_D = 0.0002637 \frac{kt}{\phi \mu c_t x_f^2} \ . \qquad \text{A.6}$$

So the equation becomes:

$$\frac{\partial^2 p_D}{\partial \epsilon^2} + \frac{\partial^2 p_D}{\partial \eta^2} = \frac{1}{2}(\cosh(2\epsilon) - \cos(2\eta)) \frac{\partial p_D}{\partial t_D} \ . \qquad \text{A.7}$$

To solve the above diffusivity equation following conditions would be used

Initial condition:

$$\lim_{t \to 0} p = p_i \, . \qquad \text{A.8}$$

In dimensionless form it is

$$\lim_{t_D \to 0} p_D = 0 \ . \qquad \text{A.9}$$

Boundary conditions are:

$$\lim_{\epsilon \to \epsilon_0} \frac{\partial p}{\partial \epsilon} = 0 \qquad \text{A.10}$$

i.e.,

$$\lim_{\epsilon \to \epsilon_0} \frac{\partial p_D}{\partial \epsilon} = 0 \ , \qquad \text{A.11}$$

$$\lim_{\epsilon \to 0} p_D = 1 \ , \ 0 \leq \eta \leq 2\pi \ , \qquad \text{A.12}$$

$$\lim_{\eta \to \frac{\pi}{2}} \frac{\partial p}{\partial \eta} = 0 \ , \qquad \text{A.13}$$

and

$$\lim_{\eta \to 0} \frac{\partial p}{\partial \eta} = 0 \ . \qquad \text{A.14}$$

Taking Laplace of diffusivity equation

$$\frac{\partial^2 p_D^-}{\partial \epsilon^2} + \frac{\partial^2 p_D^-}{\partial \eta^2} = \frac{s}{2}(\cosh(2\epsilon) - \cos(2\eta)) p_D^- \ . \qquad \text{A.15}$$

Laplace of initial and boundary conditions is

$$\lim_{t_D \to 0} p_D^- = 0 \,, \qquad \text{A.16}$$

$$\lim_{\epsilon \to \epsilon_0} \frac{\partial p_D^-}{\partial \epsilon} = 0, \ 0 \leq \eta \leq 2\pi \,, \qquad \text{A.17}$$

and

$$\lim_{\epsilon \to 0} p_D^- = \frac{1}{s}, \ 0 \leq \eta \leq 2\pi \,. \qquad \text{A.18}$$

To solve the diffusivity equation we would use the method of separation of variables which can be given as

$$\mathrm{p_D^-} = X(\epsilon)H(\eta) \ . \qquad \text{A.19}$$

Using this in equation A.13 we get

$$\frac{1}{X}\frac{\partial^2 X}{\partial \epsilon^2} - \frac{s}{2}\cosh(2\epsilon) = -\frac{1}{H}\frac{\partial^2 H}{\partial \eta^2} - \frac{s}{2}\cos(2\eta) = a \quad . \qquad \text{A.20}$$

This gives us two separate ordinary differential equations:

$$\frac{\partial^2 H}{\partial \eta^2} + \left(a + \frac{s}{2}\cos(2\eta)\right) H = 0 \qquad \text{A.21}$$

and

$$\frac{\partial^2 X}{\partial \epsilon^2} + \left(a + \frac{s}{2}\cos h(2\epsilon)\right) X = 0 \,. \qquad \text{A.22}$$

These equations has solutions in terms of modified Mathieu functions. Therefore for the ODE of H equation we take π as the period and select the even function

$$\mathrm{H_n}(\eta) = ce_{2n}(\eta, -\tfrac{s}{4}) \,, \qquad \text{A.23}$$

where

$$\mathrm{ce_{2n}}\left(\eta, -\frac{s}{4}\right) = (-1)^n \sum_{r=0}^{\infty} (-1)^r A_{2r}^{2n} \cos(2r\eta) \quad . \qquad \text{A.24}$$

Now to solve for the outer boundary condition equation A.15 of no-flow boundary, two types of Mathieu functions satisfy this boundary condition. So solution to X can be given as

$$X_n(\epsilon) = B_n Fek_{2n}\left(\epsilon, -\frac{s}{4}\right) + D_n Ce_{2n}(\epsilon, -\frac{s}{4}) \quad . \qquad \text{A.25}$$

Now applying the boundary condition equation A.15 we get

$$\mathrm{B_n}\, Fek'_{2n}\left(\epsilon, -\frac{s}{4}\right) + D_n Ce'_{2n}\left(\epsilon, -\frac{s}{4}\right) = 0 \,, \qquad \text{A.26}$$

thus

$$\mathrm{B_n} = -\frac{D_n Ce'_{2n}\left(\epsilon, -\frac{s}{4}\right)}{Fek'_{2n}\left(\epsilon, -\frac{s}{4}\right)} \quad . \qquad \text{A.27}$$

To calculate D_n we use the inner boundary condition A.18 to yield the final solution

$$\begin{aligned} p_D^-(\epsilon,\eta) = \sum_{n=0}^{\infty} \frac{(-1)^n 2A_0^{2n}}{s} \; & ((\mathrm{Fek}'_{2n}\left(\epsilon_0, -\frac{s}{4}\right) Ce_{2n}\left(\epsilon, -\frac{s}{4}\right) \\ & - Ce'_{2n}\left(\epsilon_0, -\frac{s}{4}\right) Fek_{2n}\left(\epsilon, -\frac{s}{4}\right)) \\ & / (\mathrm{Fek}'_{2n}\left(\epsilon_0, -\frac{s}{4}\right) Ce_{2n}\left(0, -\frac{s}{4}\right) \\ & - Ce'_{2n}\left(\epsilon_0, -\frac{s}{4}\right) Fek_{2n}\left(0, -\frac{s}{4}\right)) \;) \; ce_{2n}\left(\eta, -\frac{s}{4}\right) \quad . \end{aligned} \qquad \text{A.28}$$

Above solution is in laplace space for constant bottomhole pressure and thus a solution for rate has to be determined and inverted to yield the full solution for elliptical flow in the case of no flow boundary.

A closed form solution for a curved surface area of an ellipse isn't available so an approximation for the same would be used which is

$$\begin{aligned} & Curved\ surface\ area\ of\ ellipse \\ & = \frac{\pi h x_f}{2} \; (2cosh\epsilon + 2sinh\epsilon)\left(1 + \frac{N^2}{4} + \frac{N^4}{64} \right. \\ & \left. + \frac{N^6}{256}\right) \; , \end{aligned} \qquad \text{A.29}$$

here

$$N = \frac{(\cosh\epsilon - \sinh\epsilon)}{\cosh\epsilon + \sinh\epsilon} \quad . \tag{A.30}$$

Based on the above curved surface area approximation q_D for the ellipse can be written as

$$q_D^- = -\frac{\cosh\epsilon + \sinh\epsilon}{2}\left(1 + \frac{N^2}{4} + \frac{N^4}{64} + \frac{N^6}{256}\right)\left(\frac{1}{\sqrt{\sinh^2\epsilon + \sin^2\eta}}\left(\frac{\partial p_D^-}{\partial\epsilon}\right)\right), \tag{A.31}$$

for $\varepsilon \rightarrow 0$ which is at the fracture.

Therefore q_D for the present case of no flow boundary and constant bottomhole pressure is

$$\begin{aligned} q_D^- &= -\frac{1}{2}\left(1 + \frac{1}{4} + \frac{1}{64} + \frac{1}{256}\right)\left(\sum_{n=0}^{\infty}\frac{(-1)^n 2A_0^{2n}}{s}\right. \\ &\left((\mathrm{Fek}'_{2n}\left(\epsilon_0, -\frac{s}{4}\right) Ce'_{2n}\left(0, -\frac{s}{4}\right) - Ce'_{2n}\left(\epsilon_0, -\frac{s}{4}\right) Fek'_{2n}\left(0, -\frac{s}{4}\right)\right) / \\ &\left(\mathrm{Fek}'_{2n}\left(\epsilon_0, -\frac{s}{4}\right) Ce_{2n}\left(0, -\frac{s}{4}\right) - Ce'_{2n}\left(\epsilon_0, -\frac{s}{4}\right) Fek_{2n}\left(0, -\frac{s}{4}\right)\right)\right) \\ &\left. ce_{2n}\left(\eta, -\frac{s}{4}\right)\right) \quad . \end{aligned} \tag{A.32}$$

The early intermediate approximation of the above equation can be given as

$$q_D^- \approx 1.2\left(\frac{e^{-\frac{3\epsilon_0}{4}}}{\left(\frac{\pi\sinh(2\epsilon_0)}{2}\right)^{-\frac{3}{8}}}\right)\left(\frac{1}{s^{\frac{5}{8}}}\right) \quad . \qquad \text{A.33}$$

The late intermediate approximation of equation A.32 can be given as

$$q_D^- \approx \left(\frac{3}{4\pi}\right)\left(\frac{1+\left(\frac{2\pi}{3}\right)e^{-\frac{3\epsilon_0}{4}}}{\left(\frac{\pi\sinh(2\epsilon_0)}{2}\right)^{-\frac{2}{3}}}\right)\left(\frac{1}{s^{\frac{1}{3}}}\right) \quad . \qquad \text{A.34}$$

Real space inversion of the equations A.33 and A.34 can be given as

$$q_D \approx 1.2\left(\frac{e^{-\frac{3\epsilon_0}{4}}}{\left(\frac{\pi\sinh(2\epsilon_0)}{2}\right)^{-\frac{3}{8}}}\right)\left(\frac{t_{Dxf}^{-\frac{3}{8}}}{\Gamma\left(-\frac{3}{8}+1\right)}\right) \qquad \text{A.35}$$

and

$$q_D \approx \left(\frac{3}{4\pi}\right)\left(\frac{1+\left(\frac{2\pi}{3}\right)e^{-\frac{3\epsilon_0}{4}}}{\left(\frac{\pi\sinh(2\epsilon_0)}{2}\right)^{-\frac{2}{3}}}\right)\left(\frac{t_{Dxf}^{-\frac{2}{3}}}{\Gamma\left(-\frac{1}{3}+1\right)}\right) \quad . \qquad \text{A.36}$$

The above equations A.35 and A.36 can be rewritten without the gamma function as

$$q_D \approx \left(\frac{8}{3\pi}\right)\left(e^{-\left(\frac{3}{4}\right)\epsilon_0}\right)\frac{t_{Dxf}^{-\frac{3}{8}}}{\left(\frac{\pi\sinh(2\epsilon_0)}{2}\right)^{-\frac{3}{8}}} \quad , \qquad \text{A.37}$$

and

$$q_D \approx \left(\frac{9}{\pi^4}\right)\left(1+\left(\frac{2\pi}{3}\right)e^{-\left(\frac{3}{4}\right)\epsilon_0}\right)\frac{t_{Dxf}^{-\frac{2}{3}}}{\left(\frac{\pi\sinh(2\epsilon_0)}{2}\right)^{-\frac{2}{3}}} \quad . \qquad \text{A.38}$$

To convert the above rate solutions for constant bottomhole pressure to a pressure solution for constant rate solution we use the convolution theorem which is

$$\bar{p_{wD}} = \frac{1}{\bar{q_D} s^2} \quad . \qquad \text{A.39}$$

Applying convolution theorem on equations A.33 and A.34 and using an identity for gamma functions which is

$$\Gamma(1-n)\Gamma(n) = \frac{\pi}{\sin(\pi n)} \, , 0 < n < 1 \, , \qquad \text{A.40}$$

we obtain the equation for p_{wD} in real space by inversion of laplace equations as

$$p_{wD} = \left(\frac{\left(\frac{\pi\sinh(2\epsilon_0)}{2}\right)^{-\frac{3}{8}}}{\left(e^{-\left(\frac{3}{4}\right)\epsilon_0}\right)}\right)\sin\left(\frac{3\pi}{8}\right)t_{Dxf}^{\frac{3}{8}} \qquad \text{A.42}$$

and

$$p_{wD} = \left(\frac{\left(\frac{\pi\sinh(2\epsilon_0)}{2}\right)^{-\frac{2}{3}}}{\left(\frac{6}{\pi^3}\right)\left(1+\left(\frac{2\pi}{3}\right)e^{-\left(\frac{3}{4}\right)\epsilon_0}\right)}\right)\sin\left(\frac{2\pi}{3}\right)t_{Dxf}^{\frac{2}{3}} \quad . \qquad \text{A.42}$$

The solution for the case of infinite reservoir and constant bottom hole pressure i.e the rate solution for elliptical flow has been derived by Kucuk and Brigham,1979 for vertical fractured well with infinite conductivity. Also finite conductivity fracture solution has been derived by Amini et al., 2007. All these solutions are in laplace space and would need numerical inversion to find solutions.

Appendix-B

Derivation of Linear flow model:

Solution to diffusivity equation for linear flow can be derived by considering flow in a single direction thus equation A.1 in X direction can be written as

$$\frac{\partial^2 p}{\partial y^2} = \frac{\phi \mu c_t}{k}\left(\frac{\partial p}{\partial t}\right) \quad . \qquad \text{B.1}$$

The initial condition in dimensionless form can be written as (The definitions of dimensionless parameters P_D and t_D remain the same as stated in equations A.5 & A.6)

$$\lim_{t_D \to 0} p_D = 0 \quad . \qquad \text{B.2}$$

The boundary conditions for constant flow rate at wellbore and no-flow reservoir boundary can be written as

$$\lim_{y_D \to 0} \frac{\partial p_D}{\partial y_D} = -1 \, , \qquad \text{B.3}$$

and

$$\lim_{y_D \to y_{eD}} \frac{\partial p_D}{\partial y_D} = 0 \, , \qquad \text{B.4}$$

where y_D is y/x_f, where xf is fracture half-length and y_{eD} is y_e/xf where y_e is reservoir boundary.

Making the diffusivity equation dimensionless yield the equation

$$\frac{\partial^2 p_D}{\partial y_D^2} = \left(\frac{\partial p_D}{\partial t_D}\right). \quad \text{B.5}$$

Now taking laplace of diffusivity equation and the boundary conditions yields

$$\frac{\partial^2 \bar{p_D}}{\partial y_D^2} = s\bar{p_D}\,, \quad \text{B.6}$$

$$\lim_{y_D \to 0} \frac{\partial \bar{p_D}}{\partial y_D} = -\frac{1}{s}\,, \quad \text{B.7}$$

and

$$\lim_{y_D \to y_{eD}} \frac{\partial \bar{p_D}}{\partial y_D} = 0\,. \quad \text{B.8}$$

The general solution for equation B.6 can be given as

$$\bar{p_D} = Aexp\left(-y_D\sqrt{s}\right) + Bexp\left(y_D\sqrt{s}\right). \quad \text{B.9}$$

Now applying boundary condition from equation B.8

$$A = \frac{Bexp\left(y_{eD}\sqrt{s}\right)}{exp\left(-y_{eD}\sqrt{s}\right)}\,. \quad \text{B.10}$$

Now applying boundary condition from equation B.7

$$-A + B = -\frac{1}{s\sqrt{s}} \quad . \qquad \text{B.11}$$

Solving equations B.10 and B.9 would give us A and B as follows:

$$A = \frac{1}{s\sqrt{s}} \frac{exp\left(y_{eD}\sqrt{s}\right)}{(\exp\left(y_{eD}\sqrt{s}\right) - exp\left(-y_{eD}\sqrt{s}\right)} \qquad \text{B.12}$$

and

$$B = \frac{1}{s\sqrt{s}} \frac{exp\left(-y_{eD}\sqrt{s}\right)}{(\exp\left(y_{eD}\sqrt{s}\right) - exp\left(-y_{eD}\sqrt{s}\right)} \quad . \qquad \text{B.13}$$

Thus the final solution for P_D^- would be

$$p_D^- = \frac{1}{s\sqrt{s}} \frac{exp\left(y_{eD}\sqrt{s}\right)exp\left(-y_D\sqrt{s}\right) + exp\left(-y_{eD}\sqrt{s}\right)exp\left(y_D\sqrt{s}\right)}{\exp\left(y_{eD}\sqrt{s}\right) - exp\left(-y_{eD}\sqrt{s}\right)} \quad . \qquad \text{B.14}$$

This solution is in laplace space and can be inverted numerically to real space.

Also a constant pressure solution can be obtained by convolution principle

$$q_D^- \, p_{wD}^- = \frac{1}{s^2} \quad . \qquad \text{B.15}$$

In the above case $P_{wD}=P_D$ for $y_D=0$ and

$$q_D = \frac{141.2qB\mu}{kh\Delta p} \quad . \qquad \text{B.16}$$

Appendix-C

Numerical inversion algorithm: Gaver Stehfest Algorithm (Villinger, H., 1985), (Stehfest, H.,1970)

Following matlab code can be used to invert functions from laplace space to real space. (Srigutomo W., 2006)

To apply the following code for present case functionname is the function P_D^- in laplace space. T is dimensionless time t_{Dxf} and L is the no of coefficients, by default for all analysis in this thesis, L was used as 10.

```
function fun1=gavsteh(functionname,t,L)

nn2 = L/2;

nn21= nn2+1;



for n = 1:L

   z = 0.0;

        for k = floor( ( n + 1 ) / 2 ):min(n,nn2)

      z = z + ((k^nn2)*factorial(2*k))/ ...

        (factorial(nn2-k)*factorial(k)*factorial(k-1)* ...

        factorial(n-k)*factorial(2*k - n));
```

```
    end

    v(n)=(-1)^(n+nn2)*z;

end



sum = 0.0;

ln2_on_t = log(2.0) / t;

for n = 1:L

    p = n * ln2_on_t;

    sum = sum + v(n) * feval(functionname,p);

end

        fun1 = sum * ln2_on_t;
```

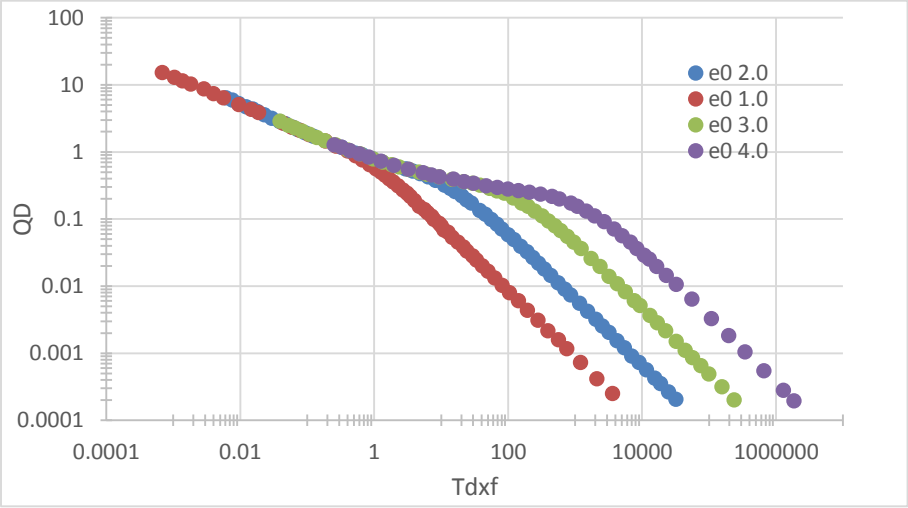

Figure C. 1: Numerical Inversion Eq A.23

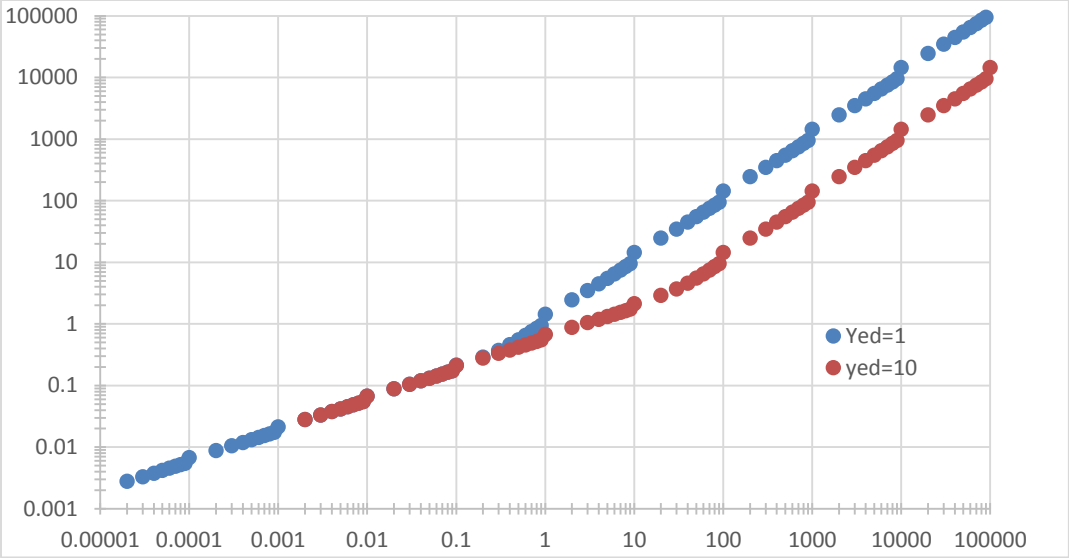

Figure C. 2: Numerical Inversion Eq B.14